

1 Title: **Monocytes and macrophages, targets of SARS-CoV-2:**
2 **the clue for Covid-19 immunoparalysis**

3
4 Running title: Covid-19 immunoparalysis of myeloid cells

5
6 Asma Boumaza^{1,2*}, Laetitia Gay^{1,2*}, Soraya Mezouar^{1,2*}, Aïssatou Bailo Diallo^{1,2},
7 Moïse Michel^{1,2}, Benoît Desnues^{1,2}, Didier Raoult^{1,2}, Bernard La Scola^{1,2}, Philippe Halfon^{1,2},
8 Joana Vitte^{1,2}, Daniel Olive³ and Jean-Louis Mege^{1,2,4#}

9
10 ¹Aix-Marseille Univ, IRD, AP-HM, MEPHI, Marseille, France

11 ²IHU-Méditerranée Infection, Marseille, France

12 ³CRCM, Inserm UMR1068, CNRS UMR7258, Institut Paoli Calmettes, Marseille, France

13 ⁴Aix-Marseille Univ, APHM, Hôpital de la Conception, Laboratoire d'Immunologie,
14 Marseille, France

15

16 * Contributed equally

17

18 **#Corresponding author :**

19 Professor Jean-Louis MEGE

20 IHU Méditerranée Infection

21 19-21, Boulevard Jean Moulin

22 13385 Marseille, France

23 Phone: (+33) 4 13 73 20 51

24 Fax: (+33) 4 13 73 20 52

25 E-mail: jean-louis.mege@univ-amu.fr

26

27 **Text word count : 3936**

28 **Abstract word count : 211**

29 **Number of figures: 5**

30 **Number of supplemental figures: 3**

31 **Number of tables: 2**

32 **Number of references: 43**

33 **Abstract**

34 To date, the Covid-19 pandemic affected more than 18 million individuals and caused more
35 than 690, 000 deaths. Its clinical expression is pleiomorphic and severity is related to age and
36 comorbidities such as diabetes and hypertension. The pathophysiology of the disease relies on
37 aberrant activation of immune system and lymphopenia that has been recognized as a
38 prognosis marker. We wondered if the myeloid compartment was affected in Covid-19 and if
39 monocytes and macrophages could be infected by SARS-CoV-2. We show here that SARS-
40 CoV-2 efficiently infects monocytes and macrophages without any cytopathic effect.
41 Infection was associated with the secretion of immunoregulatory cytokines (IL-6, IL-10,
42 TGF- β) and the induction of a macrophagic specific transcriptional program characterized by
43 the upregulation of M2-type molecules. In addition, we found that *in vitro* macrophage
44 polarization did not account for the permissivity to SARS-CoV-2, since M1- and M2-type
45 macrophages were similarly infected. Finally, in a cohort of 76 Covid-19 patients ranging
46 from mild to severe clinical expression, all circulating monocyte subsets were decreased,
47 likely related to massive emigration into tissues. Monocytes from Covid-19 patients exhibited
48 decreased expression of HLA-DR and increased expression of CD163, irrespective of the
49 clinical status. Hence, SARS-CoV-2 drives circulating monocytes and macrophages inducing
50 immunoparalysis of the host for the benefit of Covid-19 disease progression.

51

52 **Keywords:** SARS-CoV-2, Covid-19, monocytes, macrophages, polarization

53 **Introduction**

54 The novel severe acute respiratory syndrome coronavirus 2 (SARS-CoV-2/2019-n-
55 CoV) emerged in Wuhan (China) at the end of 2019 and caused the coronavirus disease of
56 2019 (Covid-19) pandemic in a few weeks, affecting more than 18 million people and killing
57 more than 690,000 to date (1). The disease is characterized by a strikingly heterogeneous
58 clinical presentation and prognosis. Most patients are pauci-symptomatic or have fever, cough
59 and fatigue, while a minority experience progression to an acute respiratory distress syndrome
60 or other critically severe conditions. The severity of the disease is related to underlying
61 conditions such as hypertension, diabetes, coronary heart diseases or obesity (2). The
62 mechanisms of the disease remain elusive at this stage, but evidence for a prominent role of
63 the immune system is accumulating. The severity of Covid-19 pneumonia is associated with
64 lymphopenia and a cytokine release syndrome (CRS) (3), which contributes to the massive
65 migration of T cells into tissues, mainly the lung as revealed by accumulation of T cells
66 within lesions (4).

67 There is evidence that myeloid cells may be involved in the pathophysiology of
68 coronavirus infection, either directly, as a targets for the virus, or indirectly, as effectors of the
69 CRS (5). Indeed, it is known from previous coronavirus outbreaks that macrophages are
70 susceptible to MERS-CoV and SARS-CoV-1 infection (6). Recently, macrophage and
71 monocyte accumulation in the alveolar lumen has been shown in a humanized mice model of
72 SARS-CoV-2 expressing human angiotensin-converting enzyme 2 (ACE2) (7). In addition,
73 SARS-CoV-2 nucleocapsid protein has been detected in lymph nodes and spleen-associated
74 CD169⁺ macrophages from Covid-19 patients (8). Finally, single cell RNA sequencing of
75 pulmonary tissue from Covid-19 patients revealed an expansion of interstitial macrophages
76 and monocyte-derived macrophages (MDM) but not of alveolar macrophages (9). However,
77 whether circulating monocytes and/or macrophages are targets of SARS-CoV-2 and whether
78 monocyte diversity is altered in Covid-19 patients require specific investigation since most
79 studies are based on this hypothesis.

80 Monocytes are innate hematopoietic cells that maintain vascular homeostasis and
81 ensure early responses to pathogens during acute infections. Three distinct human monocyte
82 subsets are described, based on the expression of CD14 and CD16 surface antigens: classical
83 CD14⁺CD16⁻ monocytes, intermediate CD14⁺CD16⁺ monocytes, and non-classical CD14⁻
84 CD16⁺ monocytes (10,11). Recently, it has been shown in murine models that classical
85 monocytes are the precursors of non-classical monocytes (12). There is evidence that

86 monocyte subsets exhibit a certain degree of functional specialization. During bacterial
87 infection, classical monocytes are recruited to the sites of inflammation, where they exert
88 typical phagocytic functions and can differentiate into inflammatory dendritic cells or
89 macrophages. Non-classical monocytes crawl along vasculature and surveil the vascular tissue
90 (13). Alterations of monocyte subset frequency have been reported in infectious and
91 inflammatory diseases (10). While macrophages largely arise from monocytes in acute
92 situations such as infection, under homeostatic conditions most tissue macrophages are of
93 embryonic origin and monocytes merely renew this population (14). Consequently, the
94 mobilization of immune cells in Covid-19 might lead to macrophage populations of multiple
95 origin in tissue lesions.

96 We show here that SARS-CoV-2 has the ability to infect human monocytes and
97 macrophages. SARS-CoV-2 infection stimulated the production of immunoregulatory
98 cytokines, interleukin (IL)-6 and IL-10 in both cell types and triggered in macrophages an
99 original transcriptional program enriched with M2-type genes. Macrophage polarization did
100 not account for permissivity to the virus since M1- and M2-polarized cells were similarly
101 infected by SARS-CoV-2. In Covid-19 patients, the numbers of classical, intermediate and
102 non-classical monocytes were decreased, irrespective of the level of severity. Their expression
103 of CD163, a molecule associated with the immunoregulatory phenotype, was significantly
104 higher than in healthy controls, whereas that of HLA-DR was decreased. Hence, SARS-CoV-
105 2 drives circulating monocytes and macrophages, inducing immunoparalysis of the host for
106 the benefit of Covid-19 disease progression.

107 **Results**

108 **SARS-CoV-2 infects monocytes and macrophages and stimulates cytokine release**

109 It has been shown that monocytes and macrophages express receptors for SARS-CoV-2 (24),
110 suggesting that the virus targets myeloid cells. We wondered whether SARS-CoV-2 was able
111 to infect human monocytes and macrophages. Monocytes, MDM and Vero cells were
112 incubated with SARS-CoV-2 strain IHU-MI3 (0.1 MOI) for 24 and 48 hours and infection
113 level was measured by RT-PCR and immunofluorescence. SARS-CoV-2 infected efficiently
114 Vero cells (Ct=18.69) after 24 hours, but a lytic process prevented the measurement of viral
115 replication, (**Figure 1A**). Monocytes were also infected after 24 hours (Ct=22.44), but the
116 viral load remained constant thereafter (Ct=22.2) (**Figure 1A**). Similarly, macrophages were
117 efficiently infected with the SARS-CoV-2 strain IHU-MI3 after 24 (Ct=22.49) and 48 hours
118 (Ct=19.67). In contrast to Vero cells, monocytes and macrophages were not uniformly
119 infected, as observed by confocal microscopy (**Figure 1A, right panel**). We next addressed
120 the ability of the IHU-MI3 strain of SARS-CoV-2 to induce the release of soluble mediators
121 from monocytes and MDMs. IL-1 β , IL-6, IL-10, TNF- α , IFN- β and TGF- β 1 levels were
122 measured in supernatants of monocytes or MDM stimulated with SARS-CoV-2 for 24 and 48
123 hours. IL-6, IL-10, and IL-1 β levels were significantly increased in stimulated monocyte
124 supernatants as compared to unstimulated conditions after 24 hours (**Figure 1B**) and were
125 persistently increased after 48 hours (**Figure 1C**), whereas no difference was observed for
126 TNF- α . In MDM supernatants, levels of IL-6 and IL-10 were increased after 24 and 48 hours
127 (**Figure 1B and C**). TGF- β levels were significantly increased in supernatants from
128 monocytes and MDMs after 48 hours of stimulation. IFN- β was never detected in
129 supernatants from monocytes or macrophages stimulated by SARS-CoV-2 (**Figure 1B and**
130 **C**). Taken together, SARS-CoV-2 infects monocytes and macrophages. The virus stimulates
131 the release of both pro- and anti-inflammatory cytokines.

132

133 **SARS-CoV-2 elicits a specific transcriptional program in macrophages**

134 Next, the expression of genes involved in the inflammatory response (*IFNA*, *IFNB*, *IFNG*,
135 *TNF*, *IL1B*, *IL6*, *IL8*, *CXCL10*) or immunoregulation, (*IL10*, *TGFB1*, *CD163*) was measured
136 by qRT-PCR in monocytes and MDM incubated with the virus for 24 and 48 hours. PCA of
137 gene expression using ClustVis software showed that unstimulated and SARS-CoV-2-
138 stimulated monocytes exhibited superimposable programs; in contrast, unstimulated and
139 SARS-CoV-2-stimulated transcriptional programs were clearly distinct in macrophages

140 (**Figure 2A**). In monocytes, a 24 hour-incubation with SARS-CoV-2 stimulated the
141 expression of the whole gene panel, but only *IFNA* gene variation reached the significance
142 level (**Figure 2B**). After 48 hours, expression of *IFNA* declined to levels of unstimulated cells
143 and there was no other change in gene expression (**Suppl figure 1**), suggesting that SARS-
144 CoV-2 was only able to activate gene expression in monocytes in a transient manner.
145 We next investigated the transcriptional program induced by SARS-CoV-2 in macrophages.
146 Similar to monocytes, at 24 hours, SARS-CoV-2 significantly increased the expression of
147 antiviral (*IFNA* and *IFNB*), inflammatory (*CXCL10* and *TNF*), and immunoregulatory genes
148 (*TGFB1* and *CD163*) (**Figure 2B**). The increase in gene expression was no longer observed
149 after 48 hours except for *TGFB* and *CD163* (**Suppl figure 1**). Hence, the early transcriptional
150 program of infected macrophages consisted of genes associated with M1 profile (type I *IFN*,
151 *CXCL10*) and M2 profile (*TGFB1* and *CD163*), suggesting that SARS-CoV-2 does not induce
152 clear polarization of macrophages at the onset of the infection but rather a delayed shift
153 toward a M2-type.

154

155 **Macrophage polarization and SARS-CoV-2 infection**

156 As SARS-CoV-2 induced an early M1/M2 followed by a late M2 program in macrophages,
157 we investigated the effect of macrophage polarization status on infection. MDM polarization
158 was induced by IFN- γ (20 ng/ml) and lipopolysaccharide (100 ng/ml) (M1), IL-4 (20
159 ng/ml) (M2), or was kept at a resting state without polarization (M0). The polarization status
160 was confirmed by measuring the expression of M1 (*IL1B*, *IL1RA*, *IL6*, *IL12*, *CXCL10*, *TNF*,
161 *NOS2*, *IFNG*) and M2 genes (*ARG1*, *IL10*, *MR*, *CD163*, *TGFB*). PCA and hierarchical
162 clustering confirmed the induction of three distinct activation statuses (**Suppl. figure 2**). The
163 expression of polarization-related genes was investigated after 24 and 48 hours of SARS-
164 CoV-2 stimulation of M1 and M2 polarized macrophages. The hierarchical clustering showed
165 that unstimulated and SARS-CoV-2-stimulated MDM (M0, M1 and M2) were present on two
166 distinct branches but the discrimination of responses as a function of polarization was not
167 possible (**Suppl figure 3**). Regarding pro- (IL-6, TNF) and anti- (IL-10, TGF- β)
168 inflammatory cytokines, SARS-CoV-2 stimulation significantly increased the release of both
169 cytokine groups in M1- and M2-polarized macrophages after 24 and 48 hours (**Figure 3A, B**).
170 In addition, no differences were observed in the viral load of M0, M1 or M2 macrophages
171 (**Figure 3C**). We next performed the same experiment using M0, M1 or M2 THP-1
172 macrophages. The choice of a cell line instead of primary macrophages aimed at minimizing

173 inter-individual variations. When THP-1 macrophages were M1 polarized, the viral load was
174 similar to that of non-polarized (M0) macrophages. In contrast, SARS-CoV-2 load was
175 significantly decreased in M2 polarized macrophages as compared with M0 macrophages
176 (**Figure 3C**). Although a type 2 immune response was associated with lesser infection of
177 macrophages, their polarization did not appear critical for SARS-CoV-2 infection.

178

179 **Monocyte subsets are altered in SARS-CoV-2-infected patients**

180 Following the demonstration of a direct *in vitro* effect of SARS-CoV-2 on monocytes and
181 macrophages, we wondered if the frequency of monocyte subsets was affected in Covid-19
182 patients. Monocyte subsets were analyzed for CD14, CD16 and HLA-DR expression by flow
183 cytometry in 76 Covid-19 patients and compared to healthy blood donors (**Figure 4A**). In the
184 latter, classical monocytes were the best represented monocyte subset (9.17% of total
185 PBMCs), while intermediate and non-classical monocytes accounted for 0.42% and 0.60%,
186 respectively. In Covid-19 patients, the percentages of classical (2.03%), intermediate (0.23%)
187 and non-classical monocytes (0.22%) were significantly lower than in healthy controls
188 (**Figure 4A**). Hence, the monocytopenia previously reported in patients infected with SARS-
189 CoV-2 (25) affected all three monocyte subsets. We wondered if circulating monocytes
190 displayed changes in the expression level of activation-associated membrane markers. Hence,
191 we measured the expression of HLA-DR, a canonical marker of monocyte activation, and
192 CD163, an immunoregulatory marker. As shown in **figure 4B**, all three monocyte subsets
193 expressed HLA-DR and CD163. In Covid-19 patients, the expression level of HLA-DR was
194 significantly decreased in intermediate and non-classical monocytes, whereas it remained
195 similar to controls in classical monocytes (**Figure 4B**). In contrast, the expression of CD163
196 was significantly increased in classical and non-classical monocytes (**Figure 4B**). The
197 opposite effect of Covid-19 on HLA-DR and CD163 expression suggests that their activation
198 status was shifted to an immunoregulatory program. This phenotypic profile of patient
199 monocytes was partly recapitulated by incubating control monocytes with SARS-CoV-2.
200 SARS-CoV-2 increased HLA-DR expression in a dose dependent manner after 24 hours and
201 decreased it after 48 hours. The inverted pattern was observed with CD163 (**Figure 4C**).
202 Finally, we wondered if the decrease in monocyte subsets and altered expression of HLA-DR
203 and CD163 reflected the severity of Covid-19. There were no significant differences in
204 monocyte phenotype among mild, moderate, and severe patients (**Figure 5**). Hence variation
205 of monocyte HLA-DR and CD163 expression in Covid-19 patients was induced by SARS-
206 CoV-2 infection, but was not related to subsequent disease severity.

207 **Discussion**

208 We showed that SARS-CoV-2 efficiently infects human monocytes and macrophages.
209 This is reminiscent of previous reports about SARS-CoV-1 that infects human macrophages
210 but does not replicate within (26). In addition, macrophages infected by SARS-CoV-1 were
211 detected in lungs of SARS patients (5). Recently, *post-mortem* examination of lymph nodes
212 and spleen revealed the presence of SARS-CoV-2 nucleocapsid protein in macrophages that
213 express CD169, a marker of macrophages from the splenic marginal zone (8). Using an
214 unsupervised computational pipeline that can detect viral RNA in any scRNA-seq data set, an
215 enrichment of SARS-CoV-2 reads in macrophages expressing secreted phosphoprotein 1 was
216 observed (27). Although monocytes and macrophages express the molecular machinery to
217 recognize and internalize SARS-CoV-2 such as ACE2, TMPRSS2 and ADAM17 (24), the
218 ability of the virus to replicate within these cells is not fully understood. Our results favor the
219 hypothesis of an abortive infection similar to SARS-CoV-1 (28) but clearly distinct from
220 MERS-CoV replication in macrophages (29).

221 The infection of monocytes and macrophages is associated with the production of
222 inflammatory cytokines that contribute to the CRS described in patients and involved in
223 disease pathogenesis. Monocytes and macrophages exhibit a common secretory profile
224 associating the release of IL-6, IL-10 and TGF- β and the absence of IFN- β . The impaired IFN
225 production is consistent with the reported inhibition of type I IFNs by SARS-CoV-1 and the
226 lack of interferon regulatory factor 3 activation in macrophages and myeloid dendritic cells
227 (5). In addition to preventing IFN- α/β responses, SARS-CoV downregulated IFN-related
228 genes in THP-1 cell lines (30). At least three SARS-CoV proteins, namely N protein, OrfB3
229 and Orf6, are known to antagonize the IFN- β response (31). While the release of IL-6 is
230 consistent with previous reports on the ability of SARS-CoV-1 to stimulate IL-6 secretion in
231 human MDM, the lack of significant changes in TNF release was not expected (26). It has
232 been shown in an *in-situ* study of *post-mortem* samples that SARS-CoV-2 induces IL-6 more
233 efficiently than TNF (8). In our hands, both monocytes and macrophages released IL-10 and
234 TGF- β , suggesting that anti-inflammatory cytokines are also involved in cell responses to
235 infection. The release of TGF- β by monocytes and macrophages may be associated with
236 tissue repair and generation of fibrosis that complicates Covid-19 evolution (32). Taken
237 together, our results suggest that the early response of monocytes and macrophages is
238 inflammatory whereas the delayed response promotes tissue repair. This model is in line with
239 the immune response unfolding in Covid-19 patients, in whom myeloid cells interact with

240 innate and adaptive immune partners able to redirect immune responses towards an
241 inflammatory status.

242 We found that SARS-CoV-2 differently affected the transcriptional programs of
243 monocytes and macrophages. In monocytes, SARS-CoV-2 elicited a transient program
244 dominated by the upregulation of IFN α gene, while macrophages exhibited a more diversified
245 transcriptional program associating inflammatory and anti-inflammatory genes, which shifted
246 to an anti-inflammatory program of M2 type. Hence, SARS-CoV-2 affected macrophage
247 polarization according to the kinetics of infection. Previous reports on SARS-CoV-1 infection
248 showed a direct effect of virus on macrophage activation. In an African green monkey model,
249 SARS-CoV-1 activated pulmonary macrophages by polarizing them toward a M1 profile
250 associated with decreased viral load but persistence of inflammation (33). In a murine model
251 of SARS-CoV-1 infection, alveolar macrophages were repolarized to limit T cell activation
252 (34). Another study revealed that SARS-CoV-1 induced non protective M2 polarization in
253 lung macrophages from infected mice(35). Whether macrophage polarization affected their
254 capacity to control SARS-CoV-2 replication was not addressed. Using polarized MDM and
255 differentiated THP-1 cells, we found that non polarized and M1 type polarized macrophages
256 were permissive to SARS-CoV-2. This may explain why obesity and diabetes, conditions
257 associated with M1 macrophage polarization, are critical comorbidities in Covid-19 (36). In
258 our hands, M2 type macrophages tended to be less permissive to SARS-CoV-2. As estrogens
259 favor M2 polarization (37), this may explain why women are less affected than men by
260 Covid-19. In addition, patients with allergic asthma seem to be less susceptible to the virus
261 (38). Our results suggest that, instead of inducing a clear polarization, SARS-CoV-2
262 exacerbates macrophage responses whatever the type of polarization.

263 The myeloid compartment was analyzed through monocyte frequencies and the
264 expression of membrane markers. Previous reports established that monocytopenia was
265 detected in Covid-19 patients in association with lymphopenia. We showed that this decrease
266 in circulating monocytes affects all monocyte subsets. There is a lack of consensus about the
267 variations of monocyte count in Covid-19, probably because of the diversity of measurement
268 tools and the heterogeneity of patients in terms of evolution. A.J. Wilk *et al* reported depletion
269 of CD16⁺ monocytes including intermediate and non-classical monocytes in a single-cell
270 RNA sequencing study of Covid-19 PBMCs (39). A Cytof study of CD45⁺ mononuclear cells
271 revealed an initial increase in cell count from mild to severe followed by a decline in more
272 severe patients (40). Expansion of IL-6 producing CD14⁺CD16⁺ monocytes was reported in

273 Covid-19 patients hospitalized in intensive care units (ICU) as compared with patients not
274 requiring ICU care (32).

275 Besides monocyte depletion in patients, remaining monocytes were characterized by a
276 down-modulation of HLA-DR and upregulation of CD163. HLA-DR down-modulation is in
277 agreement with previous studies. A. Gatti *et al* reported downregulation of monocyte HLA-
278 DR in patients with severe SARS-CoV-2 (41). A sc-RNA seq study revealed that genes
279 encoding class II HLA molecules were downmodulated in Covid-19 patients(39). P. Bost
280 reported a disease-severity-associated signature in MDM in which MHC II and type I IFN
281 genes were downmodulated (27). Another study showed that CD14⁺ monocytes maintained
282 the expression of HLA-DR in mild/moderate patients, with down-modulation occurring only
283 in severe forms (42). Previously unreported CD163 upregulation in Covid-19 patients
284 suggests a monocyte polarization toward a M2-type profile. Immunohistochemical staining of
285 SARS pneumonia demonstrated CD163⁺ M2 macrophages *in situ* (43). M2 polarization is the
286 consequence of the release of immunoregulatory cytokines, but also of the interaction with the
287 virus. Indeed, we showed a trend in monocytes infected with SARS-CoV-2 with an increase
288 in CD163 expression paralleling low HLA-DR expression. It is known that IL-6 antagonizes
289 HLA-DR expression and the addition of the specific inhibitor of IL-6 pathway, tocilizumab,
290 partially restores HLA-DR expression of CD14⁺ monocytes from Covid-19 patients (42). A
291 synergism between SARS-CoV-2 and IL-6 is likely necessary to down-modulate the
292 expression of HLA-DR and to disarm microbicidal competence of monocytes and
293 macrophages.

294 Here, we showed that SARS-CoV-2 infects monocytes and macrophages without
295 cytopathic effect and induces a more sustained activation program in macrophages. Monocyte
296 and macrophage response to SARS-CoV-2 is more complex than expected from the
297 observation of CRS, to which they poorly contribute. The investigation of circulating
298 monocytes suggested that massive migration to tissues had occurred and remaining blood
299 monocytes exhibit a repairing profile. This observation may help understand the risk of post-
300 Covid-19 complication including fibrosis. Indeed, a subset of macrophages with a pro-fibrotic
301 program has been described in patients with Covid-19 (32). The lack of correlation between
302 monocyte count and monocyte functional polarization with severity stages suggest that
303 monocytes are markers of SARS-CoV-2 infection. It is likely that other membrane markers of
304 myeloid cells are modulated according to disease progression and reflect more accurately the
305 inflammatory context associated with the severity. Taken together, our study showed that

306 monocytes and macrophages are targets of SARS-CoV-2, and their manipulation may open
307 the way for therapeutic perspectives.

308 **Methods**

309 ***Patients and ethical statement***

310 Seventy-six consecutive patients with SARS-CoV-2 infection confirmed through reverse
311 transcriptase-polymerase chain reaction (RT-PCR, Life Technologies, Carlsbad, CA, USA)
312 from March 16 through March 27, 2020 at the University Hospitals of Marseille, France, were
313 included. Not later than 48 hours post-diagnosis, patients underwent clinical laboratory tests
314 and blood was drawn through venipuncture into EDTA anticoagulated tubes.
315 Epidemiological, demographic, clinical, laboratory and outcome data were obtained from a
316 retrospective, non-interventional review of the medical charts and laboratory results.
317 Demographic characteristics of the study population are presented in **table 1**. This study was
318 performed on excess EDTA-anticoagulated total blood samples. According to French law, the
319 patients had received information that their excess samples and clinical data might be used for
320 research purposes, and retained the right to oppose (15,16).

321

322 **Cell isolation**

323 Peripheral blood mononuclear cells (PBMCs) were isolated from the blood of Covid-19
324 patients and from buffy coats from healthy blood donors (Convention N°7828, “Etablissement
325 Français du Sang”, Marseille, France) by density gradient centrifugation using Ficoll
326 (Eurobio, Les Ulis, France) as previously described (17). Monocytes were purified by CD14
327 selection using MACS magnetic beads (Miltenyi Biotec, Bergisch Glabach, Germany) and
328 cultured in Roswell Park Memorial Institute medium-1640 (RPMI, Life Technologies,
329 Carlsbad, CA, USA) containing 10% inactivated human AB-serum, 2 mM glutamine (Sigma
330 Aldrich, Saint-Quentin-Fallavier, France), 100 U/mL penicillin and 50 µg/mL streptomycin
331 (Life Technologies). After 3 days, the medium was replaced by RPMI-1640 containing 10%
332 fetal bovine serum (FBS, Life Technologies) and 2 mM glutamine, and cells were
333 differentiated into macrophages for 4 additional days. For some experiments, THP-1
334 macrophages were used and cultured in RPMI-1640 containing 10% FBS, 2mM glutamine
335 and 100 U/mL penicillin and 50 µg/mL streptomycin and differentiated into macrophages
336 after treatment with 50 ng/ml phorbol-12-myristate 13-acetate (PMA, Sigma Aldrich) for 48
337 hours (18,19).

338

339 **Virus production and cell infection**

340 SARS-CoV-2 strain IHU-MI3 was obtained after Vero E6 cells (American type culture
341 collection ATCC® CRL-1586™) infection in Minimum Essential Media (MEM) (Life
342 Technologies) supplemented with 4% FBS as previously described (20).
343 Cells were infected with 50 µl virus suspension (0.25, 0.5 or 0.1 multiplicity of infection
344 (MOI)) for 24 or 48 hours at 37°C in the presence of 5% CO₂ and 95% air in a humidified
345 incubator.

346

347 **Immunofluorescence**

348 After a 24 or 48-hour infection, cells were incubated in blocking buffer (Phosphate buffer
349 saline (PBS) supplemented with 5% FBS and 0.5% Triton X-100) for 30 minutes and washed
350 before incubation with an anti-SARS-CoV-2 spike protein antibody (Life Technologies).
351 Nuclei and F-actin were stained using DAPI and Phalloidin (Life Technologies) respectively.
352 Pictures were obtained using an LSM800 Airyscan confocal microscope (Zeiss) and a 63X oil
353 objective.

354

355 **Viral RNA extraction and q-RTPCR**

356 Viral RNA was extracted from infected cells using NucleoSpin® Viral RNA Isolation kit
357 (Macherey-Nagel, Hoerd, France) following the manufacturer's recommendations. Virus
358 detection was performed using One-Step RT-PCR SuperScript™ III Platinum™ Kit (Life
359 Technologies). Thermal cycling was achieved at 55°C for 10 minutes for reverse
360 transcription, pursued by 95°C for 3 minutes and then 45 cycles at 95°C for 15 seconds and
361 58°C for 30 seconds using a LightCycler 480 Real-Time PCR system (Roche, Rotkreuz,
362 Switzerland). The primers and the probes were designed against the E gene (20).

363

364 **RNA isolation and q-RTPCR**

365 Total RNA was extracted from monocytes or macrophages (2.10⁶ cells/well) using the
366 RNeasy Mini Kit (Qiagen, Courtaboeuf, France) and DNase I treatment to eliminate DNA
367 contaminants (21). The quality and quantity were evaluated using a spectrophotometer
368 (Nanodrop Technologies, Wilmington, USA). Reverse transcription of isolated RNA was
369 performed using a Moloney murine leukemia virus-reverse transcriptase kit (Life
370 Technologies) and oligo(dT) primers. q-PCR was performed using the Smart SYBRGreen fast
371 Master kit (Roche Diagnostics, Meylan, France) and a CFX Touch RTPCR Detection System
372 (Bio-Rad, Marnes-la-Coquette, France) using specific primers (**Table 2**). The results were
373 normalized using the housekeeping endogenous control *actb* gene encoding β-actin and are

374 expressed as relative expression of investigated genes using the formula $2^{-\Delta Ct}$ where $\Delta Ct =$
375 $Ct_{Target} - Ct_{Actin}$ as previously described (22). The threshold cycle (Ct) was defined as the
376 number of cycles required to detect the fluorescent signal.

377

378 **Immunoassays**

379 Cell supernatants were collected and the release of IL-10, tumor necrosis factor (TNF)- α , IL-
380 1 β , interferon (IFN)- β , transforming growth factor (TGF)- β 1 (R&D Systems, Bio-Techne,
381 Novel Châtillon sur Seiche, France) and IL-6 (Clinisciences, Nanterre, France) was quantified
382 using specific immunoassay kits. The sensitivity of the assays was (pg/ml) 15.4 for IL-6, 3.9
383 for IL-10, 5.5 for TNF- α , 0.125 for IL-1 β , 50 for IFN- β and 4.61 for TGF- β 1.

384

385 **Flow cytometry**

386 PBMCs from healthy donors or Covid-19 patients were resuspended in PBS (Life
387 Technologies) containing 5% FBS and 2mM EDTA (Sigma-Aldrich) for 20 minutes before
388 staining using the following fluorochrome-conjugated antibodies (mouse IgG1): CD3
389 (UCHT1), CD20 (B9E9), CD14 (RMO52), CD16 (3G8) purchased from Beckman Coulter,
390 Paris, France; HLA-DR (G46-6) and CD163 (GHI/61) from BD Biosciences, Le Pont de
391 Claix, France, and appropriate isotype controls. A minimum of 50,000 events were acquired
392 for each sample using a BD Canto II instrument (BD Biosciences) and data were analyzed
393 with FlowJo software (Tree Star, Ashland, OR).

394

395 **Statistical analysis**

396 Statistical analysis was performed with GraphPad Prism (7.0, La Jolla, CA), using the two-
397 way ANOVA test for viral quantification (Ct values) and transcriptional analysis,
398 nonparametric Kruskal-Wallis test for group comparison, nonparametric Mann-Whitney *U*
399 test for cytokine levels, and nonparametric t-test for flow cytometry results with monocyte
400 populations and surface marker expression. Turkey's and Sidak's tests were used for post-hoc
401 comparisons. qRT-PCR data for monocytes and macrophages, including principal component
402 analysis (PCA) and hierarchical clustering of gene expression, were analyzed using the
403 ClustVis webtool (23). Differences were considered statistically significant at $P < 0.05$.

404 **Authorship contributions**

405 A.B, L.G, S.M, A.B.B, M.M and J.V performed the experiments and analyzed the data. S.M,
406 B.D, D.R, B.L.S, P.H, J.V, D.O and J.L.M supervised the work. S.M, J.V and J.L.M wrote the
407 paper. All the authors read and approved the final manuscript.

408 **Acknowledgments**

409

410 Dr. Corinne Brunet, Pr. Françoise Dignat-George and Dr. Romaric Lacroix, for assistance
411 with immunophenotyping and sample tracking. Asma Boumaza was supported by the
412 "Fondation Méditerranée Infection". Soraya Mezouar was first supported by the "Fondation
413 pour la Recherche Médicale" postdoctoral fellowship (reference: SPF20151234951) and then
414 by the "Fondation Méditerranée Infection". This work was supported by the French
415 Government under the "Investissements d'avenir" (investments for the future) program
416 managed by the "Agence Nationale de la Recherche" (reference: 10-IAHU-03). The team
417 "Immunity and Cancer" was labeled "Equipe FRM DEQ 201 40329534" (for DO). This work
418 was supported by the IMMUNO-COVID project managed by the "Agence Nationale de la
419 Recherche" Flash Covid (reference: IMMUNO-COVID).

420

421 **Disclosure of conflicts of interest**

422 J.V reports speaker and consultancy fees from Thermo Fisher Scientific, Meda Pharma
423 (Mylan), Beckman Coulter, Sanofi, outside the submitted work. D.O is cofounder and
424 shareholder of Imcheck Therapeutics Emergence Therapeutics and Alderaan. The other
425 authors declare that they have no competing interests.

426 **References**

- 427 1. [https://gisanddata.maps.arcgis.com/apps/opsdashboard/index.html#/bda7594740](https://gisanddata.maps.arcgis.com/apps/opsdashboard/index.html#/bda7594740fd40299423467b48e9ecf6)
428 [fd40299423467b48e9ecf6](https://gisanddata.maps.arcgis.com/apps/opsdashboard/index.html#/bda7594740fd40299423467b48e9ecf6).
- 429 2. Zhou F, Fan G, Liu Z, Cao B. SARS-CoV-2 shedding and infectivity – Authors’ reply.
430 *The Lancet* (2020) **395**:1340. doi:10.1016/S0140-6736(20)30869-2
- 431 3. Moore JB, June CH. Cytokine release syndrome in severe COVID-19. *Science* (2020)
432 **368**:473–474. doi:10.1126/science.abb8925
- 433 4. Xu Z, Shi L, Wang Y, Zhang J, Huang L, Zhang C, Liu S, Zhao P, Liu H, Zhu L, et al.
434 Pathological findings of COVID-19 associated with acute respiratory distress syndrome.
435 *Lancet Respir Med* (2020) **8**:420–422. doi:10.1016/S2213-2600(20)30076-X
- 436 5. Dandekar AA, Perlman S. Immunopathogenesis of coronavirus infections: implications
437 for SARS. *Nat Rev Immunol* (2005) **5**:917–927. doi:10.1038/nri1732
- 438 6. Channappanavar R, Perlman S. Pathogenic human coronavirus infections: causes and
439 consequences of cytokine storm and immunopathology. *Semin Immunopathol* (2017)
440 **39**:529–539. doi:10.1007/s00281-017-0629-x
- 441 7. Bao L, Deng W, Huang B, Gao H, Liu J, Ren L, Wei Q, Yu P, Xu Y, Qi F, et al. The
442 pathogenicity of SARS-CoV-2 in hACE2 transgenic mice. *Nature* (2020)
443 doi:10.1038/s41586-020-2312-y
- 444 8. chen yongwen, Feng Z, Diao B, Wang R, Wang G, Wang C, Tan Y, Liu L, Wang C, Liu
445 Y, et al. The Novel Severe Acute Respiratory Syndrome Coronavirus 2 (SARS-CoV-2)
446 Directly Decimates Human Spleens and Lymph Nodes. *Infectious Diseases (except*
447 *HIV/AIDS)* (2020). doi:10.1101/2020.03.27.20045427
- 448 9. Liao M, Liu Y, Yuan J, Wen Y, Xu G, Zhao J, Chen L, Li J, Wang X, Wang F, et al. The
449 landscape of lung bronchoalveolar immune cells in COVID-19 revealed by single-cell
450 RNA sequencing. *Allergy and Immunology* (2020). doi:10.1101/2020.02.23.20026690
- 451 10. Narasimhan PB, Marcovecchio P, Hamers AAJ, Hedrick CC. Nonclassical Monocytes in
452 Health and Disease. *Annu Rev Immunol* (2019) **37**:439–456. doi:10.1146/annurev-
453 immunol-042617-053119
- 454 11. Passlick B, Flieger D, Ziegler-Heitbrock HW. Identification and characterization of a
455 novel monocyte subpopulation in human peripheral blood. *Blood* (1989) **74**:2527–2534.
- 456 12. Patel AA, Zhang Y, Fullerton JN, Boelen L, Rongvaux A, Maini AA, Bigley V, Flavell
457 RA, Gilroy DW, Asquith B, et al. The fate and lifespan of human monocyte subsets in
458 steady state and systemic inflammation. *J Exp Med* (2017) **214**:1913–1923.
459 doi:10.1084/jem.20170355
- 460 13. Guilliams M, Mildner A, Yona S. Developmental and Functional Heterogeneity of
461 Monocytes. *Immunity* (2018) **49**:595–613. doi:10.1016/j.immuni.2018.10.005

- 462 14. Bassler K, Schulte-Schrepping J, Warnat-Herresthal S, Aschenbrenner AC, Schultze JL.
463 The myeloid cell compartment-cell by cell. *Annu Rev Immunol* (2019) **37**:269–293.
464 doi:10.1146/annurev-immunol-042718-041728
- 465 15. LOI n° 2012-300 du 5 mars 2012 relative aux recherches impliquant la personne
466 humaine. (2012).
- 467 16. Décret n° 2016-1537 du 16 novembre 2016 relatif aux recherches impliquant la personne
468 humaine. (2016).
- 469 17. Mezouar S, Omar Osman I, Melenotte C, Slimani C, Chartier C, Raoult D, Mege J-L,
470 Devaux CA. High concentrations of serum soluble E-cadherin in patients with Q fever.
471 *Front Cell Infect Microbiol* (2019) **9**:219. doi:10.3389/fcimb.2019.00219
- 472 18. Chanput W, Mes JJ, Savelkoul HFJ, Wichers HJ. Characterization of polarized THP-1
473 macrophages and polarizing ability of LPS and food compounds. *Food Funct* (2013)
474 **4**:266–276. doi:10.1039/C2FO30156C
- 475 19. Daigneault M, Preston JA, Marriott HM, Whyte MKB, Dockrell DH. The identification
476 of markers of macrophage differentiation in PMA-stimulated THP-1 cells and
477 monocyte-derived macrophages. *PloS One* (2010) **5**:e8668.
478 doi:10.1371/journal.pone.0008668
- 479 20. Andreani J, Le Bideau M, Dufлот I, Jardot P, Rolland C, Boxberger M, Wurtz N, Rolain
480 J-M, Colson P, La Scola B, et al. In vitro testing of combined hydroxychloroquine and
481 azithromycin on SARS-CoV-2 shows synergistic effect. *Microb Pathog* (2020)
482 **145**:104228. doi:10.1016/j.micpath.2020.104228
- 483 21. Mezouar S, Vitte J, Gorvel L, Ben Amara A, Desnues B, Mege J-L. Mast cell cytonemes
484 as a defense mechanism against *Coxiella burnetii*. *mBio* (2019) **10**:e02669-18.
485 doi:10.1128/mBio.02669-18
- 486 22. Mezouar S, Benammar I, Boumaza A, Diallo AB, Chartier C, Buffat C, Boudjarane J,
487 Halfon P, Katsogiannou M, Mege J-L. Full-term human placental macrophages
488 eliminate *Coxiella burnetii* through an IFN- γ autocrine loop. *Front Microbiol* (2019)
489 **10**:2434. doi:10.3389/fmicb.2019.02434
- 490 23. Metsalu T, Vilo J. ClustVis: a web tool for visualizing clustering of multivariate data
491 using Principal Component Analysis and heatmap. *Nucleic Acids Res* (2015) **43**:W566-
492 570. doi:10.1093/nar/gkv468
- 493 24. Abassi Z, Knaney Y, Karram T, Heyman SN. The lung macrophage in SARS-CoV-2
494 infection: A friend or a foe? *Front Immunol* (2020) **11**:1312.
495 doi:10.3389/fimmu.2020.01312
- 496 25. Fan BE, Chong VCL, Chan SSW, Lim GH, Lim KGE, Tan GB, Mucheli SS, Kuperan P,
497 Ong KH. Hematologic parameters in patients with COVID-19 infection. *Am J Hematol*
498 (2020) **95**: doi:10.1002/ajh.25774
- 499 26. Tseng C-TK, Perrone LA, Zhu H, Makino S, Peters CJ. Severe acute respiratory
500 syndrome and the innate immune responses: modulation of effector cell function without

- 501 productive infection. *J Immunol Baltim Md 1950* (2005) **174**:7977–7985.
502 doi:10.4049/jimmunol.174.12.7977
- 503 27. Bost P, Giladi A, Liu Y, Bendjelal Y, Xu G, David E, Blecher-Gonen R, Cohen M,
504 Medaglia C, Li H, et al. Host-Viral Infection Maps Reveal Signatures of Severe COVID-
505 19 Patients. *Cell* (2020) **181**:1475-1488.e12. doi:10.1016/j.cell.2020.05.006
- 506 28. Yilla M, Harcourt BH, Hickman CJ, McGrew M, Tamin A, Goldsmith CS, Bellini WJ,
507 Anderson LJ. SARS-coronavirus replication in human peripheral
508 monocytes/macrophages. *Virus Res* (2005) **107**:93–101.
509 doi:10.1016/j.virusres.2004.09.004
- 510 29. Zhou J, Chu H, Li C, Wong BH-Y, Cheng Z-S, Poon VK-M, Sun T, Lau CC-Y, Wong
511 KK-Y, Chan JY-W, et al. Active replication of Middle East respiratory syndrome
512 coronavirus and aberrant induction of inflammatory cytokines and chemokines in human
513 macrophages: implications for pathogenesis. *J Infect Dis* (2014) **209**:1331–1342.
514 doi:10.1093/infdis/jit504
- 515 30. Hu W, Yen Y-T, Singh S, Kao C-L, Wu-Hsieh BA. SARS-CoV Regulates Immune
516 Function-Related Gene Expression in Human Monocytic Cells. *Viral Immunol* (2012)
517 **25**:277–288. doi:10.1089/vim.2011.0099
- 518 31. Hu Y, Li W, Gao T, Cui Y, Jin Y, Li P, Ma Q, Liu X, Cao C. The Severe Acute
519 Respiratory Syndrome Coronavirus Nucleocapsid Inhibits Type I Interferon Production
520 by Interfering with TRIM25-Mediated RIG-I Ubiquitination. *J Virol* (2017) **91**:e02143-
521 16, e02143-16. doi:10.1128/JVI.02143-16
- 522 32. Merad M, Martin JC. Pathological inflammation in patients with COVID-19: a key role
523 for monocytes and macrophages. *Nat Rev Immunol* (2020) **20**:355–362.
524 doi:10.1038/s41577-020-0331-4
- 525 33. Clay C, Donart N, Fomukong N, Knight JB, Lei W, Price L, Hahn F, Van Westrienen J,
526 Harrod KS. Primary severe acute respiratory syndrome coronavirus infection limits
527 replication but not lung inflammation upon homologous rechallenge. *J Virol* (2012)
528 **86**:4234–4244. doi:10.1128/JVI.06791-11
- 529 34. Zhao J, Zhao J, Van Rooijen N, Perlman S. Evasion by Stealth: Inefficient Immune
530 Activation Underlies Poor T Cell Response and Severe Disease in SARS-CoV-Infected
531 Mice. *PLoS Pathog* (2009) **5**:e1000636. doi:10.1371/journal.ppat.1000636
- 532 35. Page C, Goicochea L, Matthews K, Zhang Y, Klover P, Holtzman MJ, Hennighausen L,
533 Frieman M. Induction of alternatively activated macrophages enhances pathogenesis
534 during severe acute respiratory syndrome coronavirus infection. *J Virol* (2012)
535 **86**:13334–13349. doi:10.1128/JVI.01689-12
- 536 36. Brufsky A. Hyperglycemia, hydroxychloroquine, and the COVID-19 pandemic. *J Med*
537 *Virol* (2020) **92**:770–775. doi:10.1002/jmv.25887
- 538 37. Villa A, Rizzi N, Vegeto E, Ciana P, Maggi A. Estrogen accelerates the resolution of
539 inflammation in macrophagic cells. *Sci Rep* (2015) **5**:15224. doi:10.1038/srep15224

- 540 38. Morais-Almeida M, Aguiar R, Martin B, Ansotegui IJ, Ebisawa M, Arruda LK,
541 Caminati M, Canonica GW, Carr T, Chupp G, et al. COVID-19, asthma, and biological
542 therapies: What we need to know. *World Allergy Organ J* (2020) **13**:100126.
543 doi:10.1016/j.waojou.2020.100126
- 544 39. Wilk AJ, Rustagi A, Zhao NQ, Roque J, Martinez-Colon GJ, McKechnie JL, Ivison GT,
545 Ranganath T, Vergara R, Hollis T, et al. A single-cell atlas of the peripheral immune
546 response to severe COVID-19. *Infectious Diseases (except HIV/AIDS)* (2020).
547 doi:10.1101/2020.04.17.20069930
- 548 40. Wang W, Su B, Pang L, Qiao L, Feng Y, Ouyang Y, Guo X, Shi H, Wei F, Su X, et al.
549 High-dimensional immune profiling by mass cytometry revealed immunosuppression
550 and dysfunction of immunity in COVID-19 patients. *Cell Mol Immunol* (2020) **17**:650–
551 652. doi:10.1038/s41423-020-0447-2
- 552 41. Gatti A, Radrizzani D, Viganò P, Mazzone A, Brando B. Decrease of non-classical and
553 intermediate monocyte subsets in severe acute SARS-CoV-2 infection. *Cytometry A*
554 (2020)cyto.a.24188. doi:10.1002/cyto.a.24188
- 555 42. Giamarellos-Bourboulis EJ, Netea MG, Rovina N, Akinosoglou K, Antoniadou A,
556 Antonakos N, Damoraki G, Gkavogianni T, Adami M-E, Katsaounou P, et al. Complex
557 Immune Dysregulation in COVID-19 Patients with Severe Respiratory Failure. *Cell*
558 *Host Microbe* (2020) **27**:992-1000.e3. doi:10.1016/j.chom.2020.04.009
- 559 43. Zeng Z, Xu L, Xie X, Yan H, Xie B, Xu W, Liu X, Kang G, Jiang W, Yuan J.
560 Pulmonary Pathology of Early Phase COVID-19 Pneumonia in a Patient with a Benign
561 Lung Lesion. *Histopathology* (2020)his.14138. doi:10.1111/his.14138
- 562

563 **Tables**

564 **Table 1. Clinical and demographic data of the study population.** Seventy-six consecutive
 565 Covid-19 patients and 41 healthy controls were analyzed. Demographic data were available
 566 for 40 healthy controls. Nonparametric Kruskal-Wallis test was used for group comparison.
 567 HC, healthy control; F, female, M, male.

Clinical status	Covid-19 patients				Healthy controls	P value
	Severe	Moderate	Mild	All		
Sample size (%)	14 (18)	21 (28)	41 (54)	76 (100)	40	
Median age (range)	73 (45-95)	56 (29-82)	53 (18-85)	58 (18-95)	40 (18-68)	<0.0001 (with HC) 0.006 (COVID groups only)
Gender (M/F)	12/2	8/13	19/22	39/37	22/18	0.03 (with HC) 0.02 (COVID groups only)
Deceased	8	0	0	0	0	<0.0001 (COVID groups only)

568

569 **Table 2. List of primers used for q-RTPCR.**

Gene	Forward primer (5'-3')	Reverse primer (5'-3')
<i>actb</i>	GGAAATCGTGCGTGACATTA	AGGAGGAAGGCTGGAAGAG
<i>TNF</i>	AGGAGAAGAGGCTGAGGAACAAG	GAGGGAGAGAAGCAACTACAGACC
<i>CXCL10</i>	GGAAATCGTGCGTGACATTA	AGGAAGGAAGGCTGGAAGAG
<i>IL1B</i>	CAGCACCTCTCAAGCAGAAAAC	GTTGGGCATTGGTGTAGACAAC
<i>IL6</i>	CCAGGAGAAGATTCCAAAGATG	GGAAGGTTTCAGGTTGTTTTCTG
<i>IL10</i>	GGGGGTTGAGGTATCAGAGGTAA	GCTCCAAGAGAAAGGCATCTACA
<i>TGFB</i>	GACATCAAAAGATAACCACTC	TCTATGACAAGTTCAAGCAGA
<i>IFNA</i>	ACAACCTCCCAGGCACAAGGGCTGT ATTT	TGATGGCAACCAGTTCCAGAAGGCTC AAG
<i>IFNB</i>	GTTCCCTTAGGATTTCCACTCTGACTA TGGTCC	GAACCTTGACATCCCTGAGGAGATTA AGCAGC
<i>IFNG</i>	GTTTTGGGTTCTCTTGGCTGTTA	ACACTCTTTTGGATGCTCTGGTC
<i>IL8</i>	CTGGCCGTGGCTCTCTTG	TTCCACGTCAAACGGTTCC
<i>CD163</i>	CGGTCTCTGTGATTTGTAACCAG	TACTATGCTTTCCCATCCATC

570

571

572 **Figure legends**

573 **Figure 1. SARS-CoV-2 infects monocytes and macrophages and stimulates cytokine**

574 **release.** Vero E6 cells, monocytes and monocyte-derived macrophages were infected with
575 SARS-CoV-2 IHU-MI3 strain (0.1 MOI) for 24 or 48 hours. **(A)** SARS-CoV-2 quantification
576 was evaluated by RT-PCR, expressed as Ct values and observed in red in infected cells, with
577 the nucleus in blue and F-actin in green (n = 3). Pictures were acquired using a confocal
578 microscope (63x). **** $P < 0.0001$ using two-way ANOVA and Turkey's test for post-hoc
579 comparisons. **(B, C)** Pro- (IFN- β , IL-6, TNF- α , IL-1 β) and anti-inflammatory (TGF- β , IL-10)
580 cytokines release was evaluated for SARS-CoV-2-infected monocytes and macrophages at
581 **(B)** 24 and **(C)** 48 hours (n=6). Values represent mean \pm standard error of the mean. * $P <$
582 0.05, ** $P < 0.01$, *** $P < 0.001$ and **** $P < 0.0001$ using Mann-Whitney U test.

583

584 **Figure 2. SARS-CoV-2 elicits a specific transcriptional program in macrophages.**

585 Monocytes and macrophages were stimulated with SARS-CoV-2 IHU-MI3 strain (0.1 MOI)
586 for 24 or 48 hours (n = 6). The expression of genes involved in the inflammatory response
587 (*IFNA*, *IFNB*, *IFNG*, *TNF*, *IL1B*, *IL6*, *IL8*, *CXCL10*) or immunoregulation (*IL10*, *TGFB1*,
588 *CDI63*) was investigated by qRT-PCR after normalization with housekeeping actin gene as
589 endogenous control. **(A)** Data are illustrated as principal component analysis obtained using
590 ClustVis webtool for uninfected and SARS-CoV-2 infected cells in red and blue respectively,
591 with round points for 24 hours and square points for 48 hours of stimulation. **(B)** Relative
592 quantity of investigated genes at 24 hours of stimulation was evaluated for monocytes (left
593 panel) and macrophages (right panel). Values represent mean \pm standard error of the mean. * P
594 < 0.05 , ** $P < 0.01$ and *** $P < 0.001$ using two-way ANOVA and Sidak's test for post-hoc
595 comparisons.

596

597 **Figure 3. Investigation of polarized macrophages in the SARS-CoV-2 response.**

598 Macrophages and PMA-differentiated THP-1 cells were polarized by treatment with IFN- γ
599 (20 ng/ml) and lipopolysaccharide (100 ng/ml) (M1), IL-4 (20 ng/ml) (M2) or without
600 agonist (M0). Polarized macrophages were stimulated for **(A)** 24 or **(B)** 48 hours with IHU-
601 MI3 SARS-CoV-2 strain and IL-6, IL-10, TNF- α and TGF- β release were evaluated in the
602 culture supernatants by ELISA (n = 3). * $P < 0.05$, ** $P < 0.01$ and *** $P < 0.001$ using Mann-
603 Whitney U test. **(C)** Virus quantification was assessed by the evaluation of the Ct values for
604 polarized SARS-CoV-2-infected macrophages (n = 3) and PMA-differentiated THP-1 cells (n

605 = 6) at 24 hours post-infection. Values represent mean \pm standard error of the mean. $*P < 0.05$
606 using two-way ANOVA and Turkey's test for post-hoc comparisons.

607

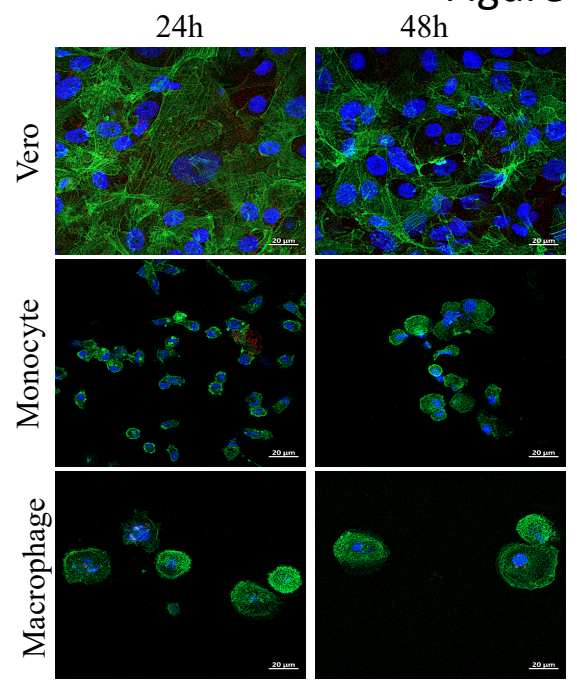
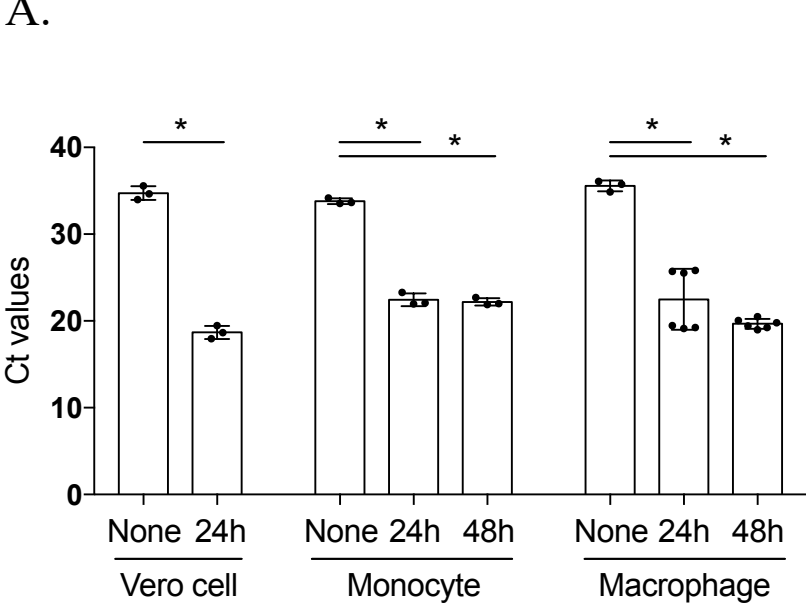
608 **Figure 4. Monocyte subsets are altered in SARS-CoV-2-infected patients.** PBMCs from
609 healthy donors and Covid-19 patients were isolated and monocyte sub-populations were
610 investigated by flow cytometry (A) Representative flow cytometry plot showing the gating
611 strategy to investigate non-classical, classical and intermediate HLA-DR⁺ monocytes from
612 Covid-19 patients and healthy donors as control. (B) Mean fluorescence intensity (MFI) of
613 HLA-DR and CD163 expression was investigated for CD14⁺, CD14⁺/CD16⁺ and CD16⁺
614 monocyte populations from healthy and Covid-19 patients. (C) Monocytes from healthy
615 donors were stimulated with SARS-CoV-2 IHU-MI3 strain (0.25 or 0.5 MOI). The expression
616 of HLA-DR and CD163 was observed at 24 and 48 hours of infection. $**P < 0.01$, $***P <$
617 0.001 and $****P < 0.0001$ using t-test.

618

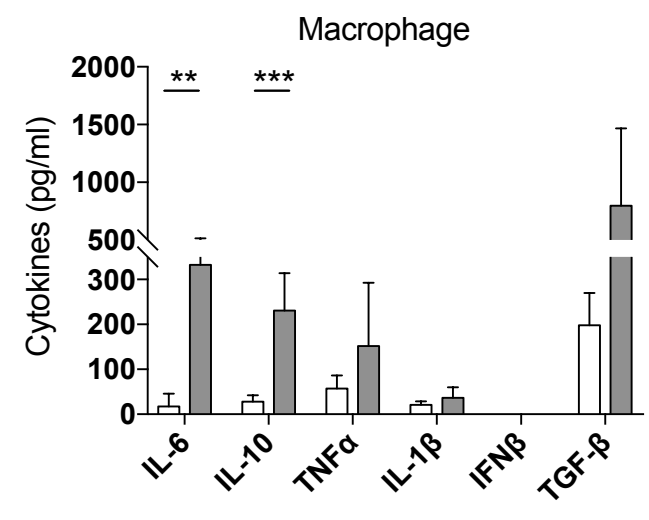
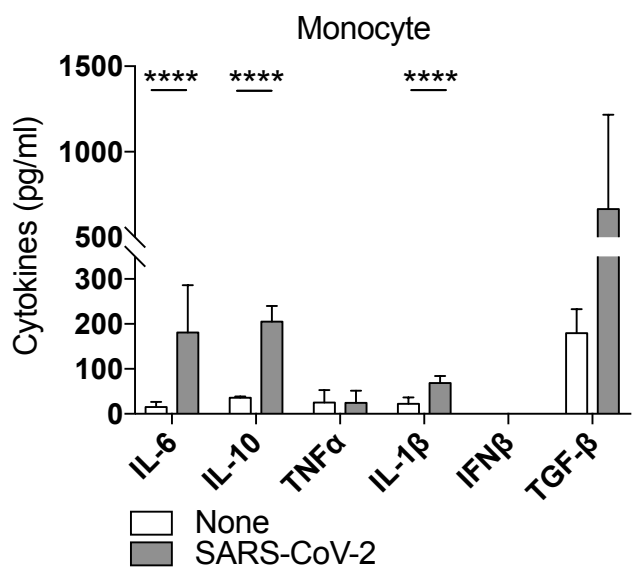
619 **Figure 5.**

620 Peripheral blood mononuclear cells from Covid-19 patients were isolated and monocyte sub-
621 populations were investigated by flow cytometry. (A) Non-classical, classical and
622 intermediate HLA-DR⁺ monocytes were evaluated from moderate, mild and severe Covid-19
623 clinical population. (B) Mean fluorescence intensity (MFI) of HLA-DR and CD163
624 expression was investigated for CD14⁺, CD14⁺/CD16⁺ and CD16⁺ monocyte populations
625 from moderate, mild and severe Covid-19 patients using t-test.

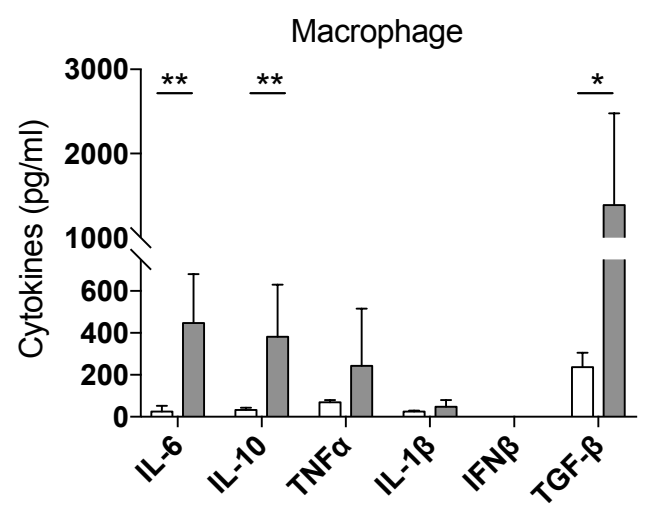
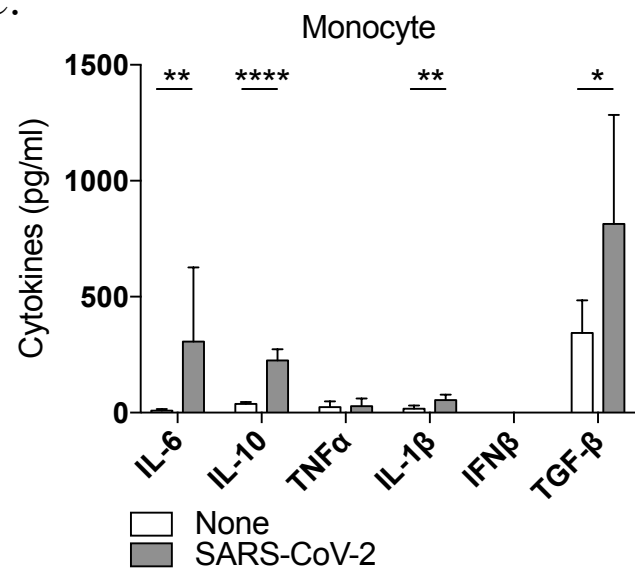
A.



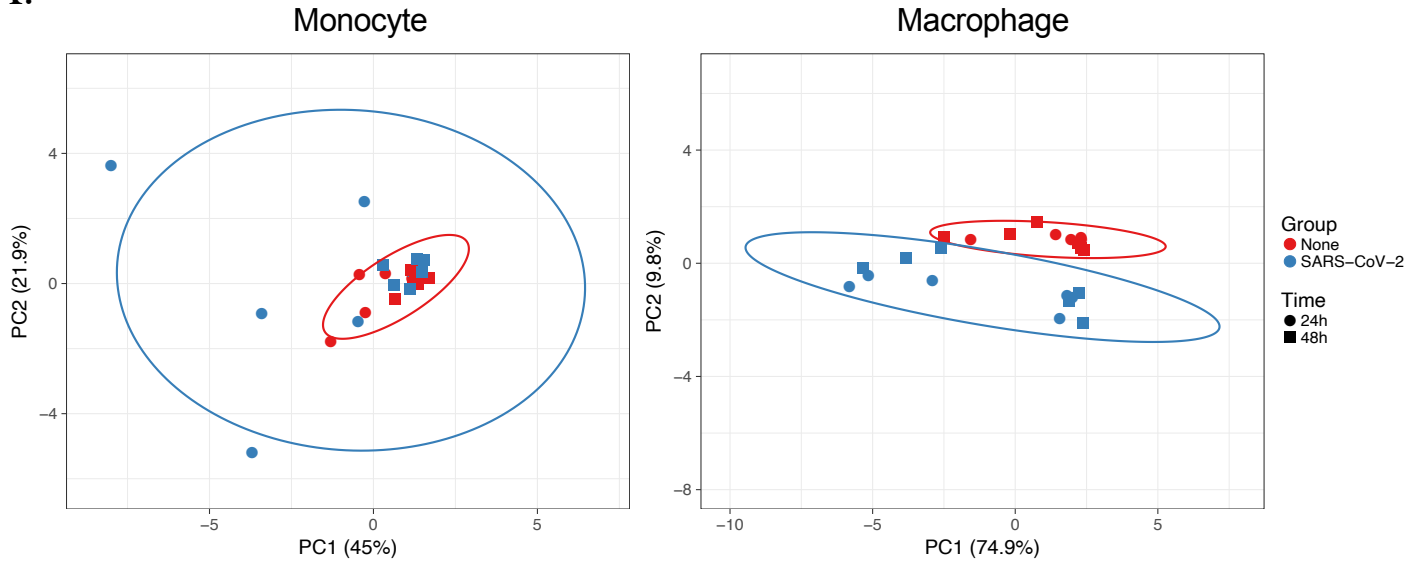
F



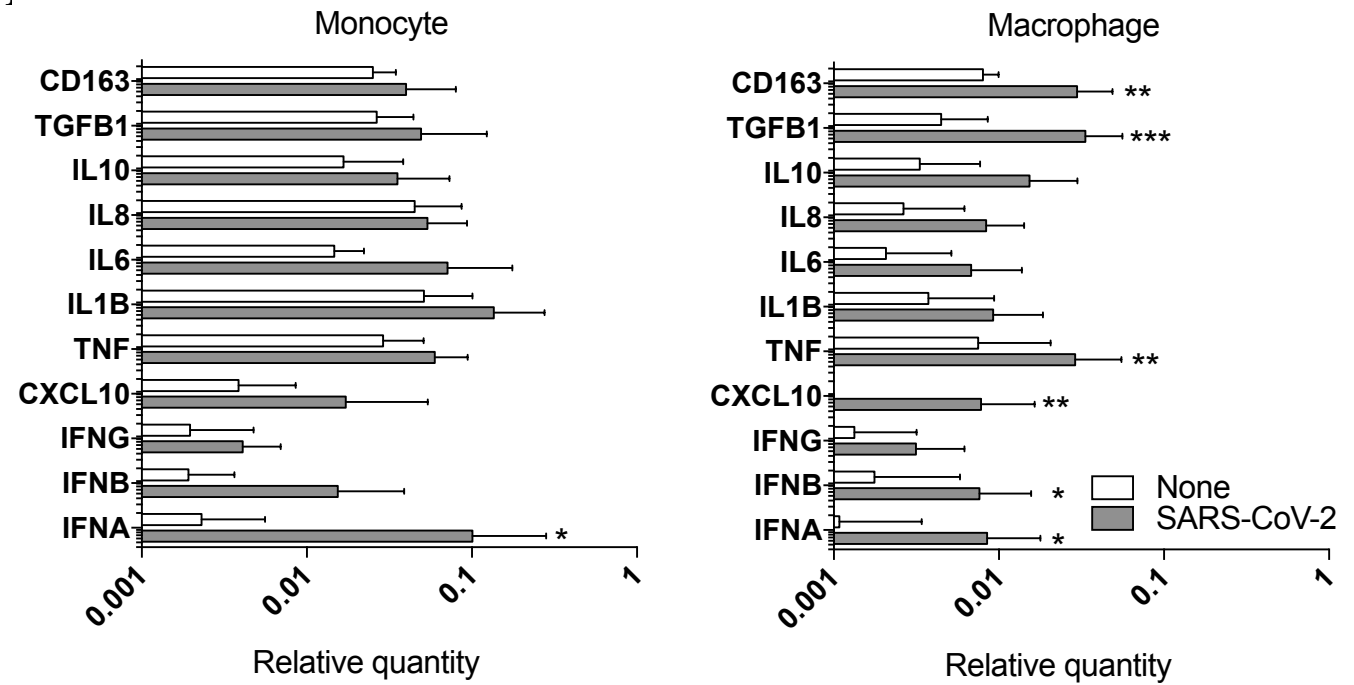
C.



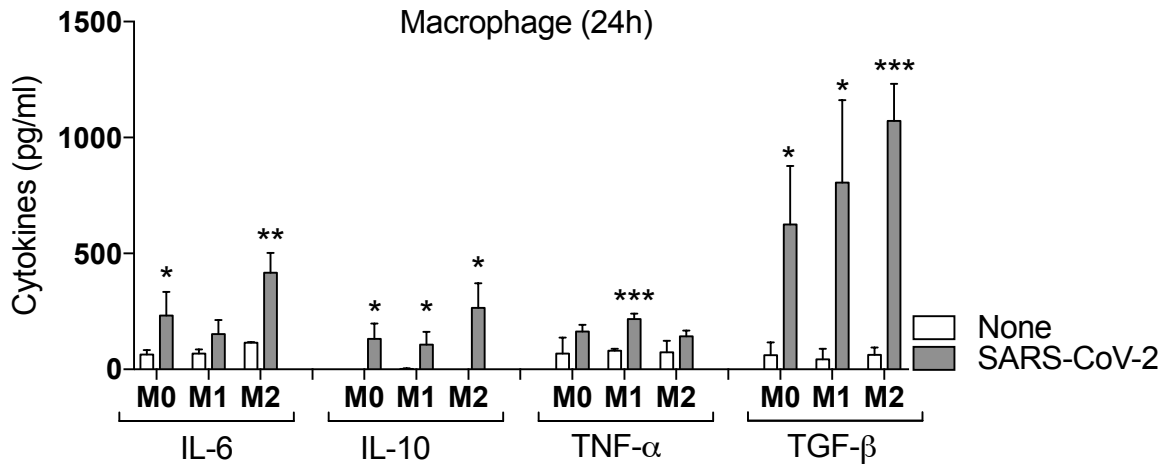
A.



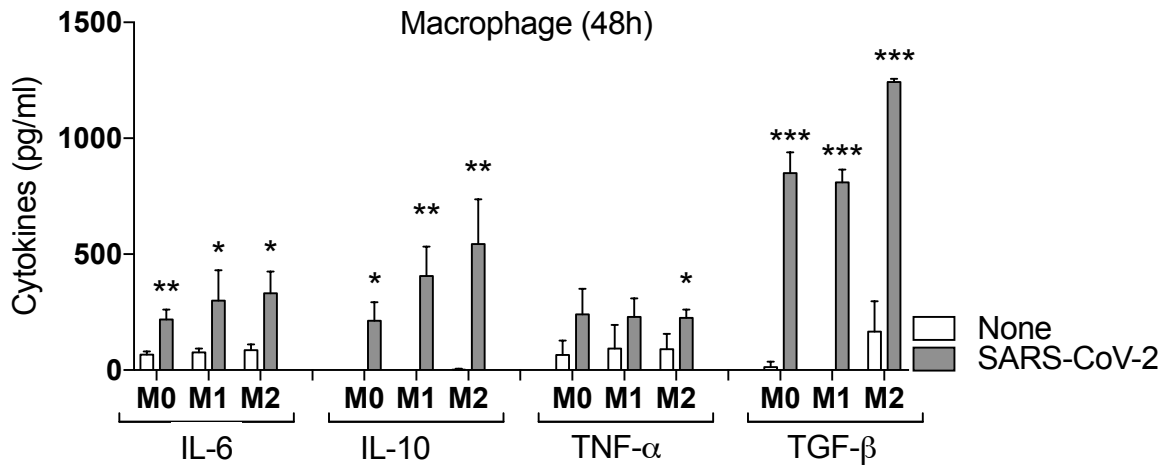
B.



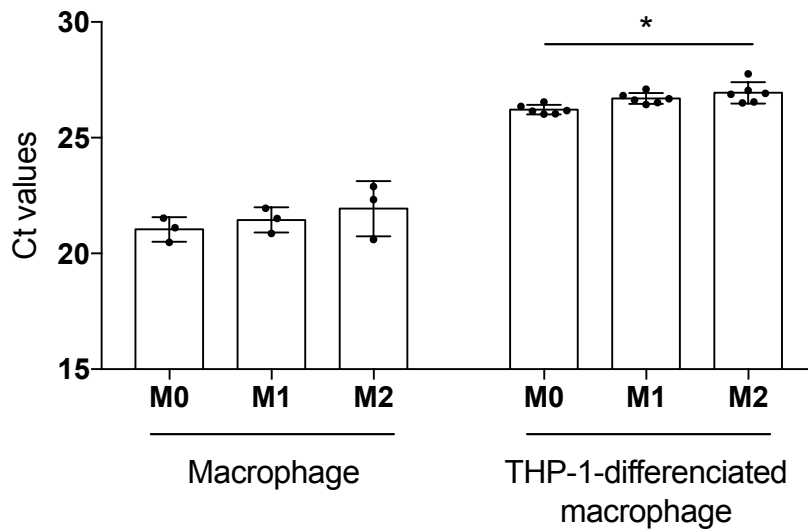
A.

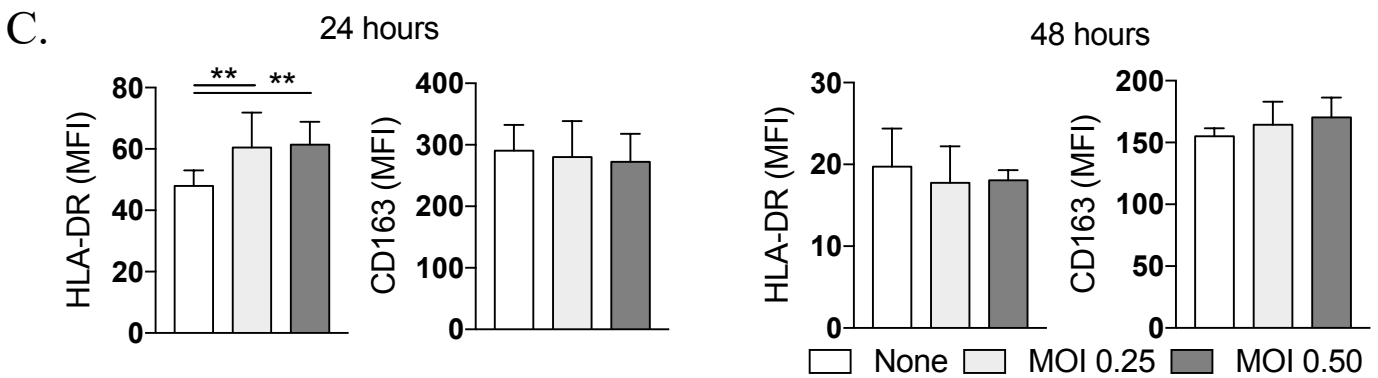
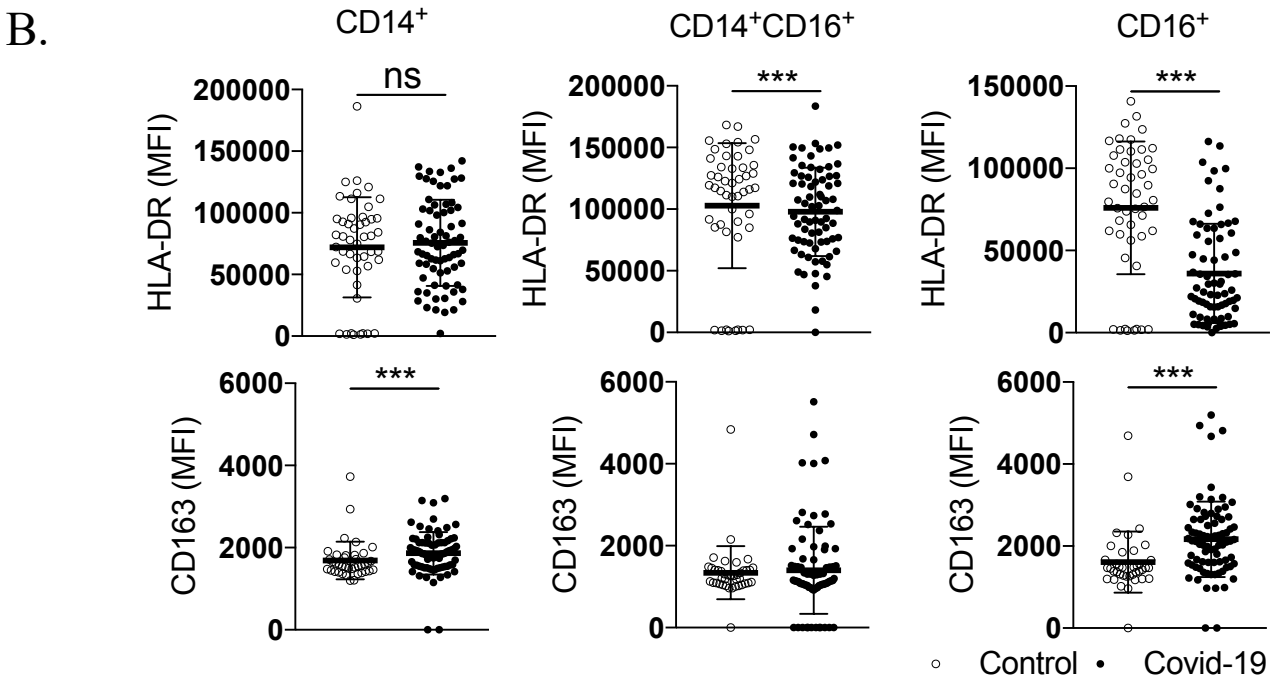
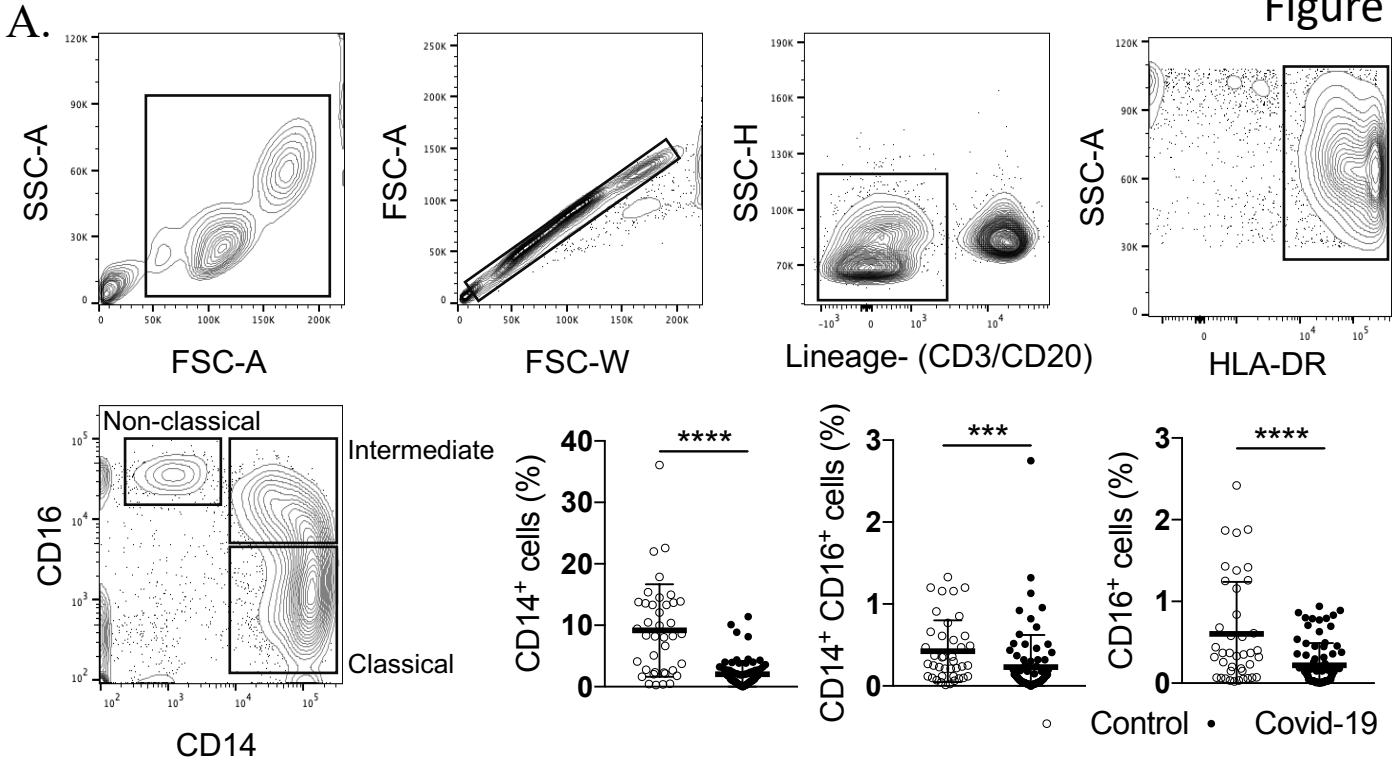


B.

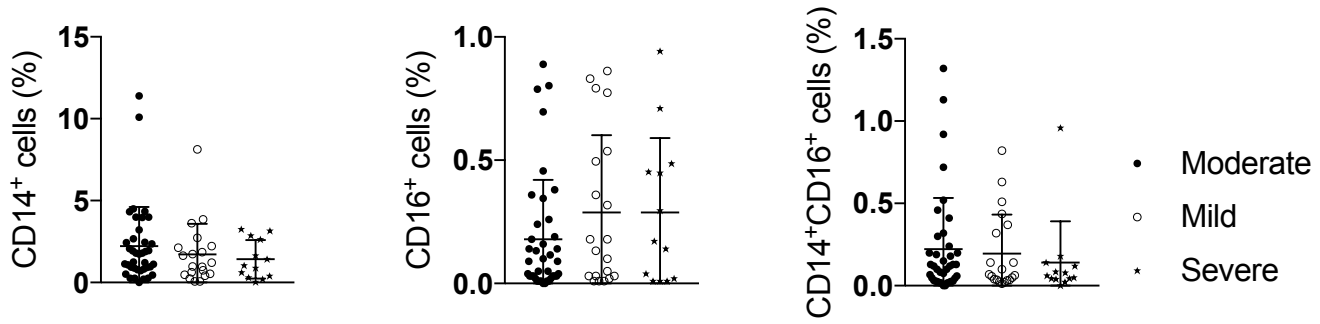


C.





A.



B.

